DOI: 10.1002/ejoc.200800252

Superacid-Catalyzed Dimerization/Cyclization of Isopropenyl-PAHs – Novel Pathways to PAH Dimers, Phenalenes and Their Stable Carbocations

Cédric Brulé,[a] Fatima Sultana,[a] Sandro Hollenstein,[a] Takao Okazaki,[a] and Kenneth K. Laali*[a]

Keywords: Polycyclic aromatic hydrocarbons / Wittig olefination / Superacids / Carbocations / Phenalenes

The isopropenyl derivatives of representative classes of polycyclic aromatic hydrocarbons (PAHs) having four and five fused-ring systems, namely pyrene, chrysene, benzo[*c*]phenanthrene (BcPh), dibenzo[*a*,*c*]anthracene (benzo[*f*]tetraphene) and perylene, were synthesized by Wittig olefination from the corresponding acetyl-PAHs. Under the influence of triflic acid (TfOH), the isopropenyl derivatives were converted to novel PAH dimers and/or phenalenes in a simple one-pot procedure. A plausible mechanism for this process has been outlined, and the synthetic scope of this chemistry has been explored. Structural features in the PAH dimers were examined by DFT. As representative initial and final carbocation intermediates in the reaction sequence, stable carbocations derived from 3-isopropenylperylene and from 4,6,6-trimethyl-6*H*-dibenzo[*a*,*kl*]anthracene were generated and studied directly by NMR spectroscopy. The NMR characteristics and charge delocalization modes in the resulting benzylic carbocations are discussed.

Introduction

In the course of studying regioisomeric α-PAH-substituted carbocations (PAH-C^+R_2) as models for PAH-epoxide ring opening,[1–4] we reported a communication[5] on the formation of 2-(phenanthren-9-yl)propan-2-carbenium ion **2** from the corresponding carbinol (Scheme 1). Upon raising temperature, **2** is easily cyclized to give the 5,6-dihydro-4*H*-benzanthracen-4-ium ion **3**, leading to the isolation of the phenalene **4** on quenching. Attempted conversion of carbinol **1** to the corresponding chloro derivative led instead to elimination and formation of the isopropenyl derivative **5**, which on treatment with FSO_3H, either in SO_2ClF or in CH_2Cl_2 at low temperature, led to clean formation of the cyclized carbocation **3**, which furnished the cyclized compound **4** upon quenching in nearly quantitative yield.[5]

Based on a number of control experiments, the mechanism outlined in Scheme 2 was proposed for this superacid-catalyzed dimerization/cyclization sequence starting from **1** or **5**.[5] Condensation of carbocation **2** (formed either by ionization of **1** or by protonation of **5**) with the isopropenyl derivative **5** (formed by elimination from **2** upon raising the temperature) serves as a key step in the formation of a dimer cation **6** (not directly detected by NMR in the stable ion experiment), which is subsequently cyclized, leading to the dimer carbocation **7**. The *ipso*-protonated dimer carbocation **8H$^+$**, formed through protonation–deprotonation equilibrium on raising the temperature, is considered a key intermediate en-route to the phenalene carbocation **3**. The relative stability of dimer **8** in the superacid and its equilibrium protonation determines the relative proportion of dimeric product **8** to phenalene product **4** (this sequence leads to a 50% maximum yield of **4** based on either **1** or **5**). Under equilibrium conditions, the carbocation **8H$^+$** formed by *ipso*-protonation yields the phenalenyl cation **3**, and subsequently the hydrocarbon **4** upon quenching. This process generates one equivalent of phenanthrene, which is protonated *in-situ* and polymerized (therefore not detected by NMR in this case). The dimer carbocation **8H$^+$** was not observed in direct stable ion studies, as it converted rapidly to the observed carbocation **3**. Therefore, no PAH dimer was isolated from compound **1** or **5** by superacid-catalysis.

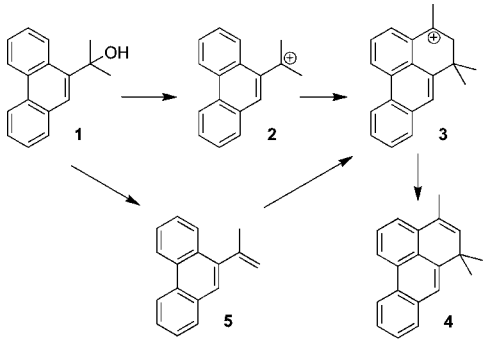

Scheme 1. Facile formation of the cyclized carbocation **3** from **1** and from **5**.

[a] Department of Chemistry, Kent State University, Kent, OH 44242, USA
Fax: +1-330-672-3816
E-mail: klaali@kent.edu
Supporting information for this article is available on the WWW under http://www.eurjoc.org or from the author.

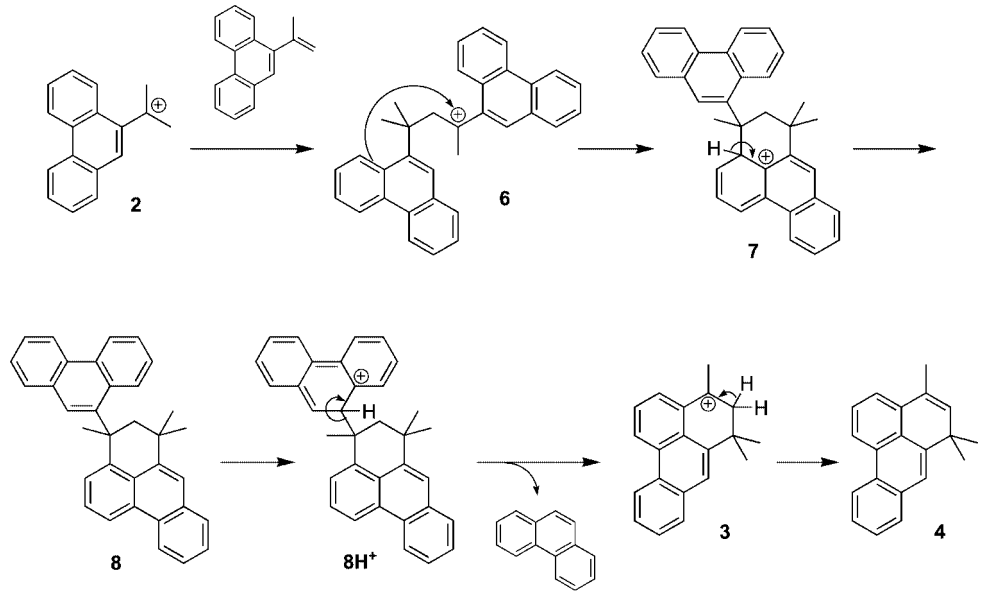

Scheme 2. Suggested mechanism for the dimerization/cyclization steps via **2** leading to **8** and **4**.

However, dimer **8** had been obtained and isolated by using $TiCl_4$ in CH_2Cl_2,[6] with no phenalene **4** being formed. Therefore, the ease of formation and relative stability of the *ipso*-protonated dimer carbocation under equilibrium conditions could determine the dimer to phenalene product ratios.

The present study sought to address the scope of this simple one-pot process as a protocol for the synthesis of novel PAH dimers and/or phenalenes from representative classes of large PAHs. Since ease of generation of the *ipso*-protonated dimer under equilibrium protonation conditions is expected to vary significantly from one PAH to another, due to variations in relative arenium ion energies, it was of interest to explore the relationship between the PAH structure and the dimer to phenalene product ratios.

Results and Discussion

Synthesis of the Isopropenyl-PAHs

The isopropenyl derivatives of 1-acetylpyrene (**9**), 4-acetylpyrene (**10**), 6-acetylchrysene (**11**), 5-acetylbenzo[*c*]phenanthrene (**12**), 10-acetyldibenzo[*a*,*c*]anthracene (**13**), and 3-acetylperylene (**14**) (see Figures 1 and 2), were successfully synthesized in reasonable yields by Wittig olefination, employing the phosphonium ylide $Ph_3P{=}CH_2$, made from methyltriphenylphosphonium bromide and sodium amide in THF. Among the acetylated derivatives, compound **13** was previously unknown. In the dibenzo[*a*,*c*]anthracene skeleton, electrophilic attack is typically directed to the *meso*-position (C-9). This has been shown in stable ion pro-

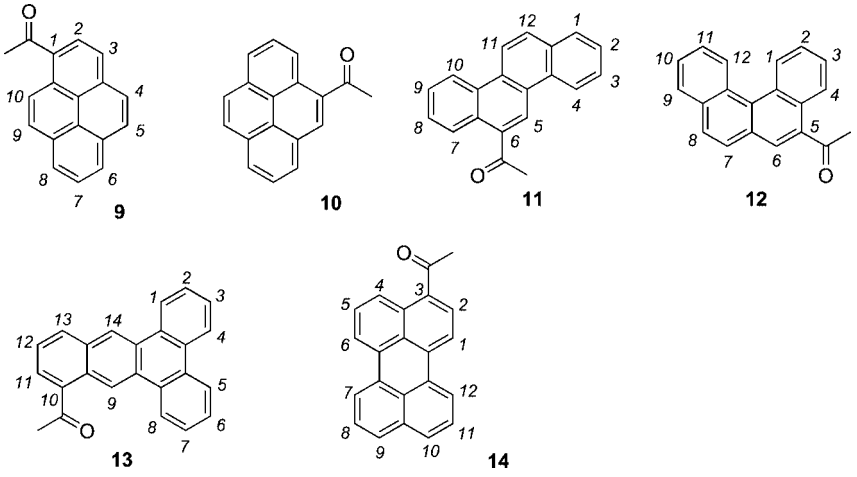

Figure 1. Acetyl-PAHs employed in the study.

tonation [6] as well as in nitration and bromination with NBS,[7] whereas bromination with Br_2 in CH_2Cl_2 led to the 10-bromo derivative.[7] In the present study, under classical Friedel–Crafts acetylation conditions ($MeCOCl/AlCl_3$), the 10-acetyl derivative **13** was obtained quantitatively. Acetylation at C-10 exerts a strong *peri*-deshielding effect on H-9, which appears as a singlet at δ = 10.26 ppm.

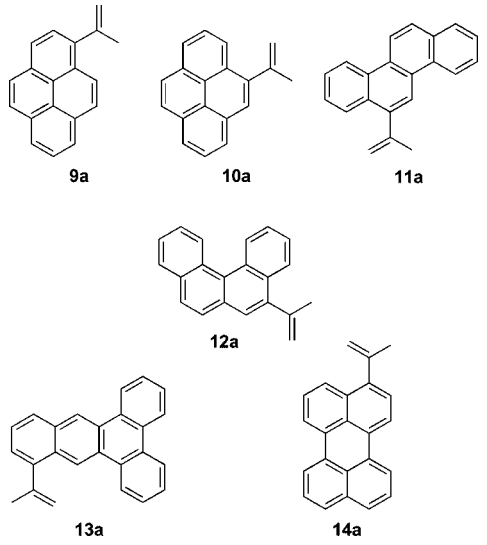

Figure 2. The synthesized isopropenyl derivatives.

Formation of the corresponding isopropenyl derivatives **9a**–**14a** was readily apparent in the ^1H NMR spectra during Wittig olefination, by the appearance of two distinct olefinic proton signals (multiplets), typically in the 5.2 to 5.6 ppm range. The NMR spectroscopic data, including specific assignments based on 2D-NMR (for **10a**–**14a**), are gathered in the Exp. Section.

Reaction of Isopropenyl-PAHs with TfOH

The isopropenyl-PAHs shown in Figure 2 were treated with TfOH in CH_2Cl_2 initially at –78 °C, and after few minutes the reaction mixtures were allowed to warm up to –10 °C. The progress of the reactions was monitored by TLC, and the reactions were quenched when no further changes in the dimer/phenalene ratios were observed under these conditions.

The 1-isopropenylpyrene **9a** gave the dimer **9b** as the main product (which was isolated), along with minor amounts of the phenalene **9c** and parent pyrene (which were detected in the NMR of the crude reaction mixture before purification) (see Scheme 3 and Figure S1–S2 in the Supporting Information). Unfortunately, it was not possible to isolate and purify compound **9c** from the mixture consisting of unreacted **9a** and parent pyrene.

The 4-isopropenylpyrene **10a** was efficiently converted to dimer **10b** as the major product along with the phenalene **10c** as the minor product (together with 1 equivalent of pyrene) (see Scheme 3 and Figure S3–S4).

Product distributions observed with **9a** and **10a** indicate that once formed, the dimer-PAHs are relatively stable in TfOH, and that the subsequent steps leading to phenalenes have relatively high activation barriers under these reaction conditions. This is unlike the situation with 9-isopropenylphenanthrene[5] (Scheme 1), whereby cyclization was rapid and no dimer survived. Based on the relative pyrenium ion stabilities[8], formation of the requisite *ipso*-protonated carbocation from **9b** (α position of pyrene) should be more favorable than **10b** (protonation at the α,β position). This appears to be consistent with the increased formation of **9c** relative to **10c** in the product mixture in the low-temperature experiments (see Scheme 3). In the case of previously studied 9-isopropenylphenanthrene,[5] the observed rapid

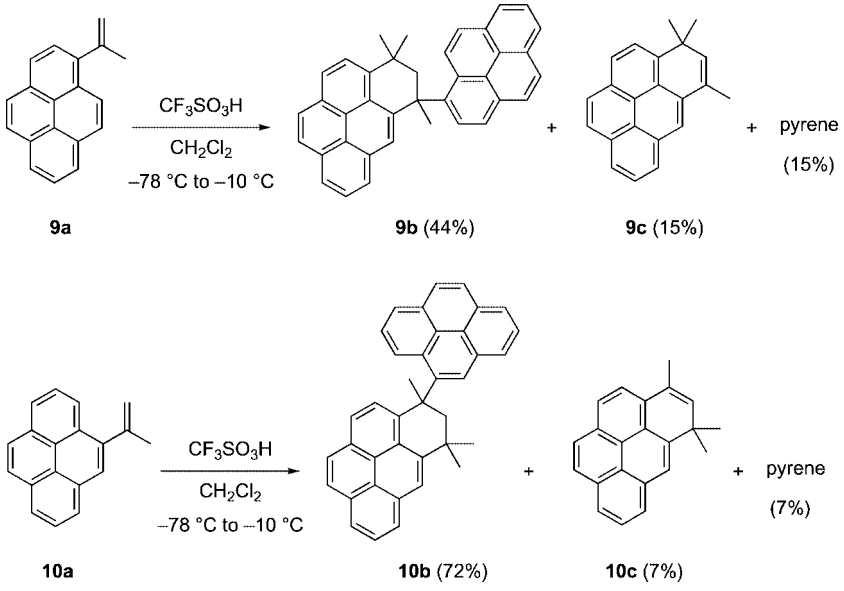

Scheme 3. Dimerization/cyclization of **9a** and **10a**.

conversion to carbocation **3** via **8H**$^+$ can be rationalized because it involves *ipso*-protonation at the *meso*-position which is energetically favorable over other alternatives.

Specific NMR assignments for the dimeric compounds **9b** and **10b** are gathered in Figure 3, along with relative stereochemistry deduced from NOE experiments.

Since attempts to grow suitable crystals from **9b** and **10b** for X-ray analysis were unsuccessful, their structures were optimized by DFT (Figure S5). In the optimized structures, the trimethylcyclohexenyl rings have envelope conformations and their axial methyl groups are close to each other. The distance between the equatorial methyl carbon and the axial hydrogen is 0.3–0.4 Å smaller than that between the equatorial methyl carbon and the equatorial hydrogen. These geometrical features are consistent with NOE experiments.

Reaction of 5-isopropenylchrysene **11a** with TfOH resulted in the formation of the corresponding phenalene **11c** in 49% yield, with only traces of the dimeric product **11b** being detected in the crude reaction mixture at completion of the reaction. Facile conversion of **11b** to **11c** reflects the favorable energetics of the chrysenium ion of protonation at C-6.[9,10] The DFT-optimized structure of **11b** is shown in Figure S5. The computed angles between the average planes of the benzene rings in the optimized structures of **9b**, **10b**, and **11b** (Table S1, Supporting Information) indicate that the pyrene and the chrysene skeletons remain planar in these dimers.

A similar reaction of 5-isopropenylbenzo[*c*]phenanthrene **12a** with TfOH resulted in the isolation of the corresponding phenalene **12c** in good yield along with benzo[*c*]phenanthrene BcPh (Scheme 4 and Figure S6–S7). No **12b** was isolated from the reaction mixture following the work-up. Facile conversion of **12b** to **12c** under equilibrium protonation conditions may be traced to the highly favorable energetics of C-5 protonation in the BcPh moiety.[10,11] The DFT-optimized structure of **12b** is shown in Figure S5. In this case, both BcPh units are severely distorted, the largest angles are found between A/D, A/C and B/D rings (see Table S1).

Reaction of 10-isopropenyldibenzo[*a*,*c*]anthracene **13a** with TfOH resulted in the isolation of the dimer **13b** in good yields, along with the cyclized phenalene **13c** as minor

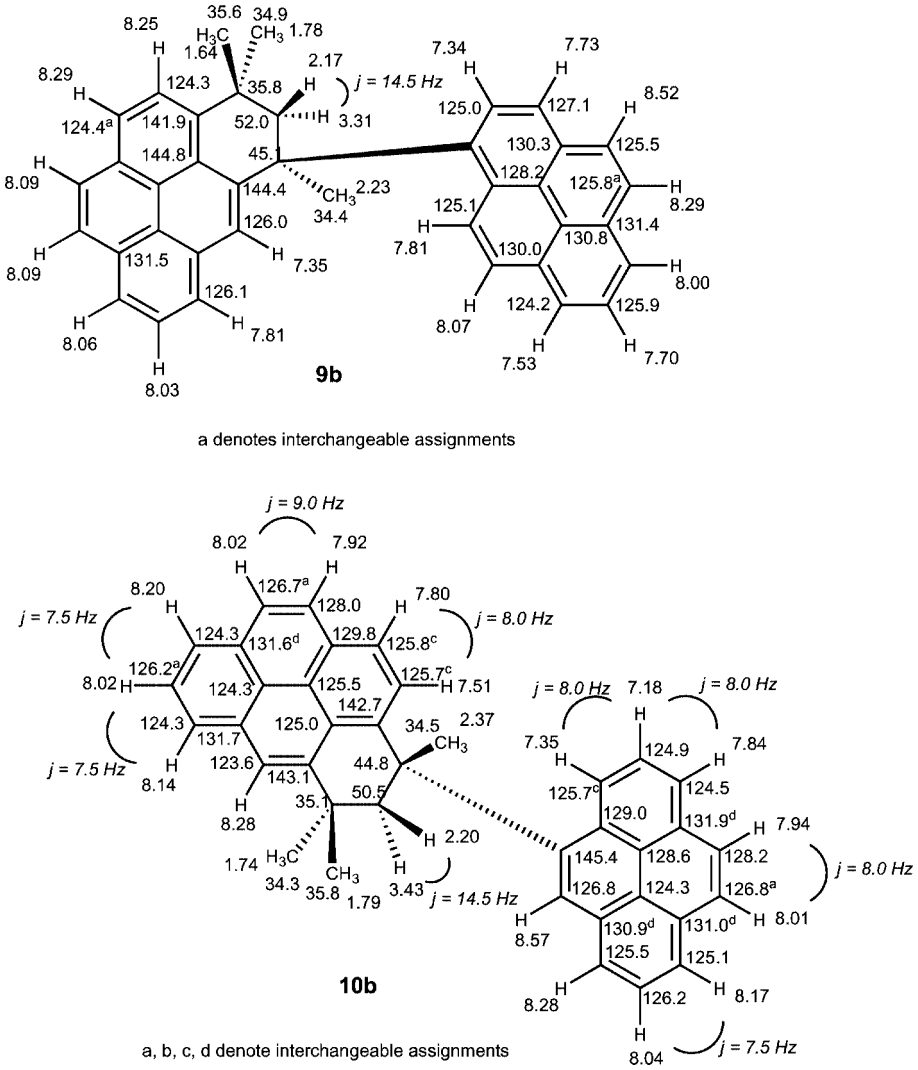

Figure 3. Specific NMR assignments (by 500 MHz NMR), including relative stereochemistry, for the dimers **9b** and **10b**.

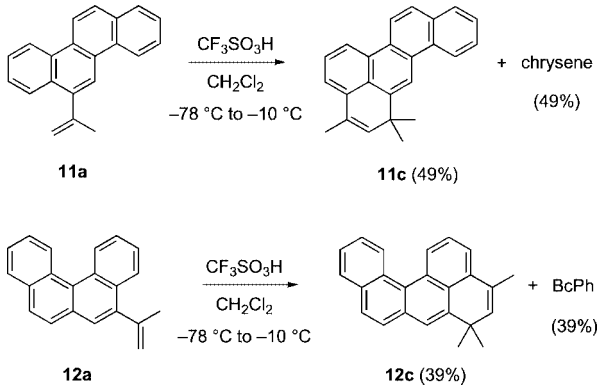

Scheme 4. Dimerization/cyclization of **11a** and **12a** (dimers **11b** and **12b** were not observed).

product (Scheme 5 and Figure S8–S9). Inefficient conversion of **13b** to **13c** could again be traced to relative arenium ion energies in the dibenzo[*a*,*c*]anthracene DBA moiety, which strongly favor protonation at the *meso*-positions (C-9/C-14),[6] therefore disfavoring the formation of the requisite *ipso*-protonated carbocation precursor to **13c**. The DFT-optimized structure of dimer **13b** is included in Figure S5. In this case, one DBA unit is severely buckled, whereas the other remains planar (see Table S1).

Reaction of 3-isopropenylperylene **14a** with TfOH resulted in the formation of dimer **14b**, with only traces of the cyclized phenalene **14c** being isolated along with perylene (see Scheme 5 and Figure S11). The DFT-optimized structure of **14b** is included in Figure S5. The computed ring angles indicate some distortion from planarity in one perylene unit (see Table S1).

Electrophilic attack in the perylene skeleton is directed to C-3/C-4/C-9/C-10.[12] Availability of unsubstituted C-4/C-9/C-10 positions in the perylene moiety of **14b** likely makes the formation of the requisite *ipso*-protonated carbocation less likely under equilibrium conditions, leading to minor formation of the phenalene **14c**.

Interestingly, it was possible to force the dimer **14b** to react further, when, in a small-scale control experiment, an authentic sample of **14b** was allowed to react with TfOH in CH_2Cl_2 and the temperature was raised up to room temp. (the color of the solution changed from deep green to deep blue). Analysis (TLC and NMR) of the reaction mixture showed that the dimer was fully consumed, and a 1:1 mixture of **14c** and perylene was formed (75% yield; see Figure S11).

Model Stable Ion Studies

a) Protonation of 3-Isopropenylperylene **14a**: Compound **14a** was cleanly protonated in FSO_3H/SO_2ClF at –78 °C to give the benzylic carbocation **14aH**$^+$. This carbocation represents the first key intermediate in the dimerization/cyclization/cleavage sequence, leading to **14b** and **14c** under equilibrium protonation conditions (see Schemes 5 and 2). Specific NMR assignments for the carbocation are included in Figure 4 along with its charge delocalization mode based on magnitude $\Delta\delta^{13}C$ values. The carbocation center is observed at δ = 191.3 ppm in the ^{13}C NMR spectroscopy.

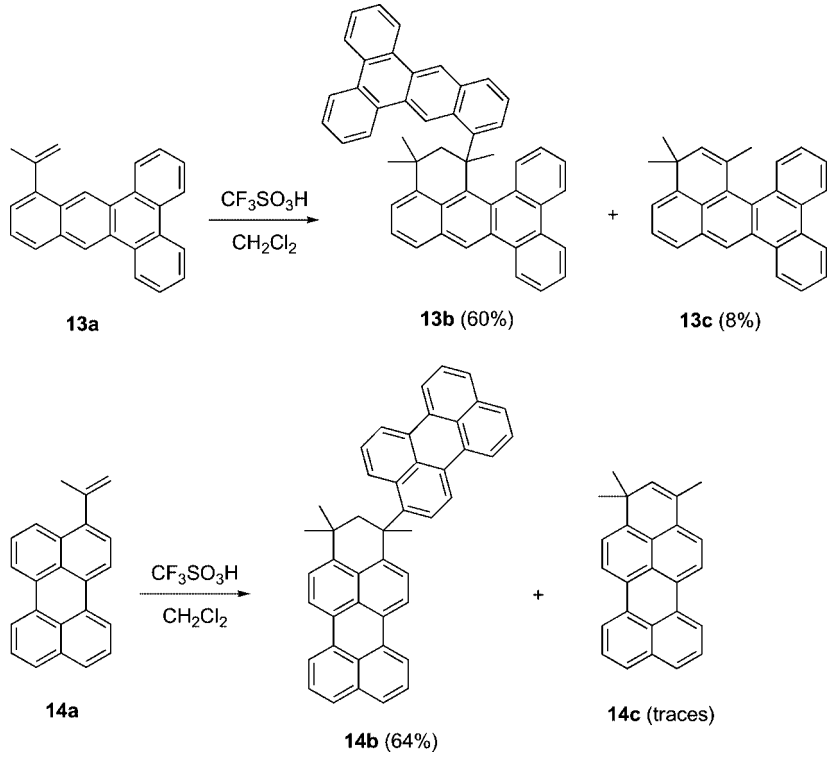

Scheme 5. Dimerization/cyclization of **13a** and **14a**.

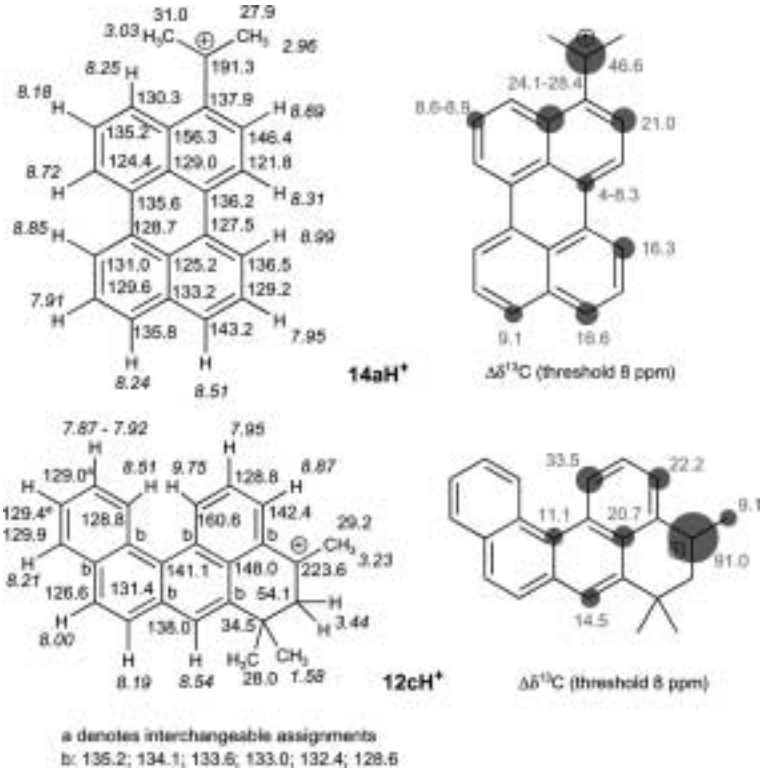

Figure 4. NMR spectroscopic data and charge delocalization modes in model carbocations **14aH**$^+$ and **12cH**$^+$ ($\Delta\delta^{13}$C relative to the corresponding neutral species **14a** and **12c**).

There is relatively extensive charge delocalization into the perylene moiety, and p–π back-bonding, i.e. the double-bond character of perylene-$C^+(Me)_2$ bond is reflected in the non-equivalence of the methyl groups (see Figure 4 and Figures S12–S13 in the Supporting Information).

b) Protonation of the Phenalene **12c** *Derived from BcPh:* Low-temperature reaction of compound **12c** with FSO_3H/SO_2ClF led to clean generation of the benzylic carbocation **12cH**$^+$. This carbocation represents the last intermediate in the reaction sequence and is the immediate precursor to the cyclic phenalene **12c** (see Schemes 4 and 2). Specific NMR assignments for the carbocation are included in Figure 4 along with its charge delocalization mode based on the magnitude of $\Delta\delta^{13}$C values. The carbocation center is observed at δ = 223.6 ppm in the ^{13}C NMR with the positive charge delocalized within a naphthalenium moiety (see Figure 4 and Figures S14–S15).

Comparative Summary

It has been shown that the isopropenyl derivatives of various classes of PAHs can be synthesized and isolated in relatively good yields by Wittig olefination of the acetyl-PAHs. These compounds react with triflic acid to produce novel PAH dimers, which can react further to furnish the corresponding phenalenes under equilibrium protonation conditions. The dimer to phenalene product ratios depend on the structure of the PAHs and on the feasibility of generation of the *ipso*-protonated dimer under equilibrium protonation conditions, which triggers subsequent cleavage, leading to the phenalene with concomitant loss of one equivalent of the parent PAH. In four of the six cases studied (**9a**, **10a**, **13a**, and **14a**) the dimer and the phenalene were both formed, but the former constituted the major product. In the case of **11a** and **12a** (via chrysene and BcPh) and the earlier studied isopropenylphenanthrene,[5] formation of the requisite *ipso*-protonated dimer is energetically more favorable and the dimers reacted quickly to produce the isolated phenalenes.

Experimental Section

General: CH_2Cl_2 was dried with CaH_2 under argon. Room temperature NMR spectra were recorded either on a Bruker Advance 400 or a Varian 500 INOVA instrument, while low-temperature NMR spectra were recorded exclusively on the Varian 500 instrument. Electrospray-MS (ES-MS) data were acquired with a Bruker Esquire-LC instrument by mixing a dilute CH_2Cl_2 solution of compound with NH_4NO_3 in CH_3CN to form the corresponding ammonium clusters $[PAH\text{-}NH_4]^+$. Infrared data were acquired on a Bruker Vector 33 spectrometer with Fourier Transform and are expressed in cm^{-1}.

The reported selectivities, given in some cases alongside the yields, are defined as yield/conversion × 100.

Computational Protocols: Structures were optimized by the density function theory (DFT) method at B3LYP/6-31G(d) level using the

Gaussian 03 package.[13,14] All computed geometries were verified by frequency calculations to have no imaginary frequencies. Energies of the optimized structures are summarized in Table S2. Structural features are summarized in Figure S5 and Table S1.

1. Acetylation Reactions

General Procedure: To a cooled suspension (0 °C, ice bath) of aluminium chloride (1.1 mmol, 1.4 equiv.) in dry CH_2Cl_2 (3 mL), acetyl chloride (0.9 mmol, 1.1 equiv.) was added. After stirring until a clear solution was obtained, a solution of the polycyclic aromatic hydrocarbon (0.8 mmol, 1.0 equiv.) in dry CH_2Cl_2 (2 mL) was slowly introduced and the reaction mixture was stirred at room temperature for 1 to 3 hours. Then the mixture was cooled to 0 °C (ice bath) and subsequently hydrolyzed with 3 mL of HCl (0.5 M). After decantation and separation, the aqueous layer was washed with CH_2Cl_2 (2×4 mL) and combined organic layers were dried with $MgSO_4$, filtered and concentrated under reduced pressure. The product was purified by silica column chromatography using CH_2Cl_2/hexane (7:3).

Compounds **9**, **10**, **11**, **12** and **14** have already been described (see ref.[4,9,11,15–17]).

10-Acetyldibenzo[*a*,*c*]anthracene (13): Quantitative yield (NMR proof). This compound was used directly in the Wittig reaction without further purification. Specific ^1H and ^{13}C NMR assignments are shown below.

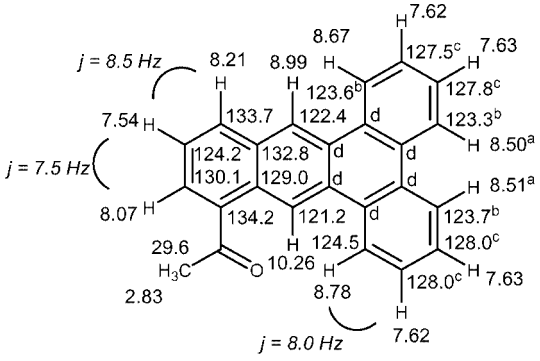

a, b, c denote interchangeable assignments
d: 130.4 (2), 130.3, 130.2, 129.6, 128.8 ppm

2. Wittig Olefination Reactions

General Procedure: A mixture of methyltriphenylphosphonium bromide (0.8 mmol, 1.4 equiv.) and sodium amide (0.8 mmol, 1.35 equiv.) was diluted in dry THF (3 mL) and stirred at room temperature under argon until a color change was seen. Then, a solution of acetylated substrate (0.6 mmol, 1.0 equiv.) in dry THF (2 mL) was added. After stirring for 2 to 4 hours, the reaction mixture was washed with brine (4 mL) and organic layer was extracted with diethyl ether (3×5 mL), dried with $MgSO_4$, filtered and the solvents evaporated under vacuum. Finally, the product was purified by column chromatography using CH_2Cl_2/hexane (3:7).

1-Isopropenylpyrene (9a): 90 mg, yield 62% (conversion 90%, selectivity 69%). ^1H NMR (500 MHz, $CDCl_3$): δ = 8.32 (d, J = 9.0 Hz, 1 H), 8.15 (d, J = 7.5 Hz, 2 H, H-6,8), 8.12 (d, J = 8.0 Hz, 1 H), 8.05 (d, J = 9.0 Hz, 1 H), 8.03 (s, 2 H), 7.98 (dd, J = 7.5, 7.5 Hz, 1 H, H-7), 7.85 (d, J = 8.0 Hz, 1 H), 5.56 (m, 1 H, CH_2), 5.17 (m, 1 H, CH_2), 2.34 (m, 3 H, Me) ppm. ^{13}C NMR (126 MHz, $CDCl_3$): δ = 145.1 (*C*Me), 140.1 (*C*CMe), 131.6 (C), 131.2 (C), 130.4 (C), 127.9 (C), 127.6 (CH), 127.4 (CH), 127.3 (CH), 126.1 (CH), 125.6 (CH), 125.4 (CH), 125.2 (C), 125.1 (2 CH), 125.0 (CH), 124.8 (CH), 117.1 (CH_2), 25.9 (Me) ppm. IR (KBr): $\tilde{\nu}$ = 3042, 2924, 1443, 838 cm^{-1}. MS (ES): m/z = 260 $[M + NH_4]^+$, 243 $[M + H]^+$.

4-Isopropenylpyrene (10a): 135 mg, yield 93%, m.p. 115–120 °C. IR (KBr): $\tilde{\nu}$ = 3045, 2922, 1467, 824, 720 cm^{-1}. MS (ES): m/z = 242 $[M^+]$. Specific ^1H and ^{13}C NMR assignments are shown below.

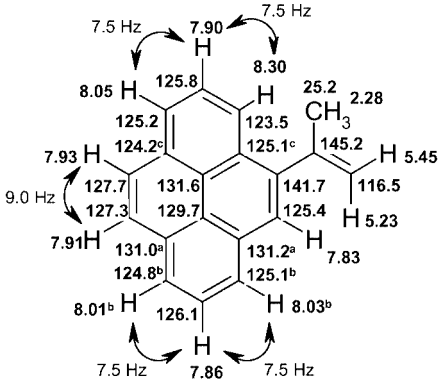

a, b, c denote interchangeable assignments

6-Isopropenylchrysene (11a): 95 mg, yield 59%; m.p. 150–155°C. Specific ^1H and ^{13}C NMR assignments are shown below.

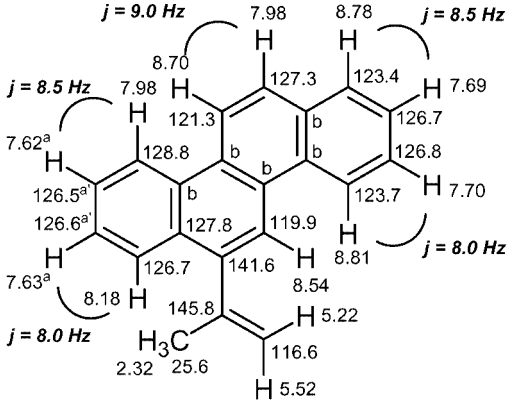

a, a' denote interchangeable assignments
b: 132.5, 131.3, 130.7, 130.4, 128.0 ppm

5-Isopropenylbenzo[*c*]phenanthrene (12a): 64 mg, yield 40% (conversion 58%, selectivity 69%). Specific ^1H and ^{13}C NMR assignments are shown below.

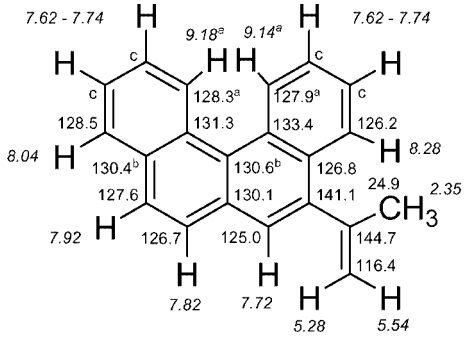

a, b denote interchangeable assignments
c: 126.1; 125.8; 125.8; 125.7

10-Isopropenyldibenzo[*a*,*c*]anthracene (13a): 122 mg, yield 64% (conversion 80%, selectivity 80%). Specific ^1H and ^{13}C NMR assignments are shown below.

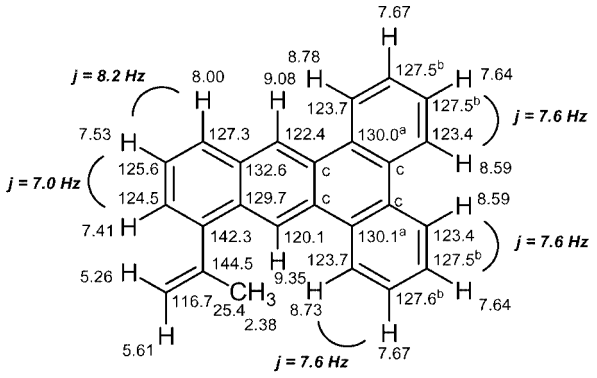

a, b denote interchangeable assignments
c: 130.4, 128.7, 128.4, 128.2 ppm

3-Isopropenylperylene (14a): 110 mg, yield 63% (conversion 86%, selectivity 74%), m.p. 170-180 °C. IR (KBr): $\tilde{\nu}$ = 3048, 2923, 810, 766 cm^{-1}. Specific ^{1}H and ^{13}C NMR assignments are shown below.

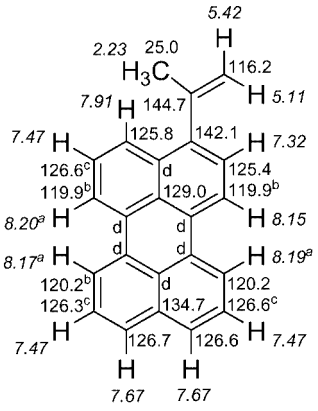

a, b, c denote interchangeable assignments
d: 132.2; 131.4; 131.3; 130.2; 128.6; 127.9

3. Dimerization–Cyclization–Cleavage Reactions

General Procedure: To a cooled (–78 °C, dry ice/acetone) solution of the isopropenylated substrate (0.1 mmol) in dry CH_2Cl_2 (2 mL) under argon was added triflic acid (2-3 drops). After 5 min of stirring at –78 °C, the reaction mixture was warmed to –10 °C (NaCl, ice). The reaction was monitored by TLC until no further reaction was observed. Then the mixture was quenched with 2 mL of KOH (10%) and extracted with CH_2Cl_2 (3 × 3 mL). The combined organic extracts were dried with $MgSO_4$, filtered and concentrated under vacuum. The resulting products were separated and purified by silica column chromatography using hexane/CH_2Cl_2 (8:2). The reported isolated yields for the phenalenes are based on the isopropenyl derivatives (50% is maximum).

3,3,5-Trimethyl-5-(pyren-1-yl)-4,5-dihydro-3*H*-benzo[*cd*]pyrene (9b): 21 mg, yield 44%. See Figure 3 for NMR spectroscopic data.

3,5,5-Trimethyl-3-(pyren-4-yl)-4,5-dihydro-3*H*-benzo[*cd*]pyrene (10b): 35 mg, yield 72%. MS (ES): *m*/*z* = 502 [M + NH_4]$^+$, 485 [M + H]$^+$. IR (KBr): $\tilde{\nu}$ = 3040, 2924, 1602, 1450, 873, 822, 724 cm^{-1}. See Figure 3 for NMR spectroscopic data.

3,5,5-Trimethyl-5*H*-benzo[*cd*]pyrene (10c): 2 mg, yield 7%. ^{1}H NMR (400 MHz, $CDCl_3$): δ = 8.13 (d, *J* = 8.0 Hz, 1 H, H-1), 8.11 (dm, *J* = 7.0 Hz, 1 H, H-7), 8.08 (s,1 H, H-6), 8.07 (dd, *J* = 8.0, 1.0 Hz, 1 H, H-9), 8.01 (dd, *J* = 8.0, 7.0 Hz, 1 H, H-8), 7.98 (m, 1 H, H-10 or H-11), 7.95 (d, *J* = 7.6 Hz, 1 H, H-11 or H-10), 7.94 (d, *J* = 8.0 Hz, 1 H, H-2), 5.91 (q, *J* = 1.4 Hz, 1 H, H-4), 2.35 (d, *J* = 1.4 Hz, 3 H, C^3Me), 1.57 (s, 6 H, C^5Me) ppm. ^{13}C NMR (101 MHz, $CDCl_3$): δ = 143.4 (C-3), 137.1 (C-4), 131.6 (C), 131.5 (C), 130.4 (C), 130.2 (C-2a), 127.5 (CH), 126.8 (CH), 126.0 (CH), 125.0 (CH), 124.3 (C), 124.2 (C), 124.1 (C), 123.9 (CH), 123.8 (CH), 123.5 (CH), 123.4 (C), 120.7 (CH), 37.5 (C-5), 33.6 (C^5CH_3), 20.0 (C^3CH_3) ppm.

4,6,6-Trimethyl-6*H*-benzo[*hi*]chrysene (11c): 15 mg, yield 49%, m.p. 170-175 °C. ES-MS: *m*/*z* = 309 [M + H]$^+$, 294 [M + H–CH_3]$^+$, 267, 253 (loss of C_4H_8). Specific ^{1}H and ^{13}C NMR assignments are shown below.

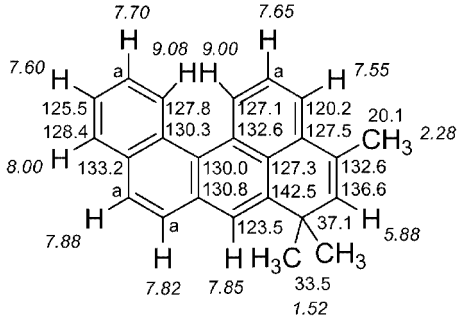

a: 126.6; 125.9; 125.6; n.d.

4,6,6-Trimethyl-6*H*-dibenzo[*a*,*kl*]anthracene (12c): 12 mg, yield 39%. Specific ^{1}H and ^{13}C NMR assignments are given below.

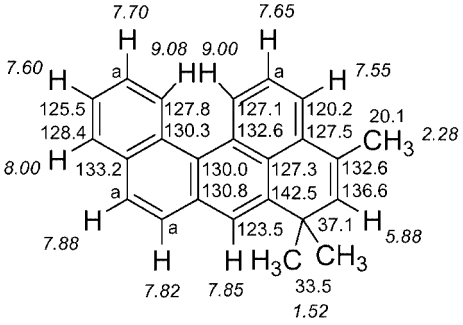

a: 126.6; 125.9; 125.6; n.d.

1,3,3-Trimethyl-1-(dibenzo[*a*,*c*]anthracen-10-yl)-2,3-dihydro-3*H*-dibenzo[*hi*,*p*]chrysene (13b): 38 mg, yield 60%. ^{1}H NMR (500 MHz, $CDCl_3$): δ = 9.72 (s, 1 H), 9.16 (s, 2 H), 9.05 (s, 1 H), 8.85 (d, *J* = 7.5 Hz, 1 H), 8.79 (m, 2 H), 8.73 (d, *J* = 8.0 Hz, 1 H), 8.67 (m, 2 H), 8.46 (d, *J* = 7.5 Hz, 1 H), 8.37 (br. d, *J* = 7.5 Hz, 1 H), 8.02 (d, *J* = 8.5 Hz, 1 H), 7.98 (d, *J* = 8.0 Hz, 1 H), 7.78–7.46 (m, 10 H), 3.18 (d, ^2J = 12.5 Hz, 1 H, CH_2), 2.64 (d, ^2J = 12.5 Hz, 1 H, CH_2), 2.19 (s, 3 H, CH_3), 1.56 (s, 6 H, CH_3) ppm. ^{13}C NMR (125 MHz, $CDCl_3$): δ = 158.0, 134.1, 133.1, 130.5, 130.4, 130.3, 130.2, 130.1, 130.0, 129.8, 129.7, 129.5, 129.3, 128.2, 128.0, 127.7, 127.6, 127.5 (2C), 127.4, 127.3 (2C), 127.2 (2C), 127.1, 125.4, 125.2, 123.6 (2C), 123.5 (2C), 123.4, 123.3, 123.1, 123.0, 121.8, 118.2, 59.8, 51.5, 45.8, 31.7, 31.4, 29.7 ppm (the signals of seven quaternay carbon atoms were not detectable).

1,3,3-Trimethyl-3*H*-dibenzo[*hi*,*p*]chrysene (13c): 3 mg, yield 8%. ^{1}H NMR (500 MHz, $CDCl_3$): δ = 9.28 (s, 1 H), 9.18 (s, 1 H), 8.79 (m, 2 H), 8.59 (m, 2 H), 8.09 (m, 1 H), 7.72–7.55 (m, 5 H), 6.30 (m, 1 H, Me_2CCH=), 2.27 (s, 3 H, CH_3), 1.57 (s, 6 H, CH_3) ppm.

1,3,3-Trimethyl-1-(perylen-3-yl)-2,3-dihydro-3*H*-benzo[*cd*]perylene (14b): 38 mg, yield 64%. ^{1}H NMR (400 MHz, $CDCl_3$): δ = 8.31 (d, J = 7.6 Hz, 1 H), 8.28 (m, 2 H), 8.21 (d, J = 7.2 Hz, 1 H), 8.12 (d, J = 7.6 Hz, 1 H), 8.03 (d, J = 7.2 Hz, 1 H), 7.99 (d, J = 7.6 Hz, 1 H), 7.92 (m, 2 H), 7.70 (m, 2 H), 7.67 (d, J = 8.4 Hz, 1 H), 7.64 (d, J = 8.0 Hz, 1 H), 7.61 (d, J = 8.0 Hz, 1 H), 7.52 (m, 1 H), 7.49 (dd, J = 8.0, 7.6 Hz, 1 H), 7.45 (dd, J = 8.0, 7.6 Hz, 1 H), 7.39 (dd, J = 8.0, 7.6 Hz, 1 H), 7.22 (d, J = 8.8 Hz, 1 H), 6.99 (dd, J = 8.4, 8.0 Hz, 1 H), 6.91 (d, J = 8.0 Hz, 1 H), 2.99 (d, J = 14.4 Hz, 1 H, CH_2), 2.06 (s, 3 H, CH_3), 1.98 (d, J = 14.4 Hz, 1 H, CH_2), 1.67 (s, 3 H, CH_3), 1.56 (s, 3 H, CH_3) ppm. ^{13}C NMR (101 MHz, $CDCl_3$): δ = 146.0, 144.4, 143.5, 134.6, 134.5, 131.8, 131.7 (2C), 131.6, 131.2, 130.4, 130.3, 129.4, 129.3, 129.0, 128.5, 128.2, 127.5, 127.4, 127.2, 127.0, 126.6 (2C), 125.7, 125.2, 123.9, 120.8, 120.7, 120.1, 119.9, 119.7, 119.6, 119.5, 49.9, 44.1, 34.9, 34.6, 33.7, 31.9 ppm (the signals of seven quaternay carbon atoms were not detectable).

1,3,3-Trimethyl-3*H*-benzo[*cd*]perylene (14c): Less than 2 mg, yield < 5%. ^{1}H NMR (400 MHz, $CDCl_3$): δ = 8.23 (d, J = 8.0 Hz, 1 H), 8.15 (m, 3 H), 7.63 (m, 2 H), 7.53 (d, J = 8.1 Hz, 1 H), 7.46 (m, 2 H), 7.36 (d, J = 8.0 Hz, 1 H), 5.81 (q, J = 1.3 Hz, 1 H), 2.20 (d, J = 1.3 Hz, 3 H), 1.54 (s, 6 H) ppm.

4. Stable Carbocation Generation from 14a and 12c

Protonation of 14a: In a 5-mm NMR tube 6 mg of 3-isopropenylperylene **14a** was introduced and tube was flushed with argon and cooled to –78 °C. About 0.3 mL of SO_2ClF was condensed into the NMR tube directly. After completion of SO_2ClF addition, 3 drops of FSO_3H were slowly added in order to prevent any local overheating. The mixture immediately turned deep-green. After vigorous stirring at –78 °C (vortex), 4–5 drops of CD_2Cl_2 were slowly introduced into the NMR tube (vortex mixing) and the sample was analyzed by NMR at –65 °C. Afterwards, the sample was warmed to –10 °C (NaCl/ice/water bath) and kept at this temperature for 30 minutes (regular vortex mixing). The sample was checked by NMR at –65 °C but no changes were detected. Then the sample was kept in a 0 °C (ice/water) for 3 hours and checked again by NMR at –65 °C. However, still no changes occurred (sample was deep green). In an attempt to observe the dimerization step directly by NMR, a tiny amount of **14a** was added to the superacid solution of **14aH$^+$** while at 0 °C, but no noticeable changes could be seen via ^{1}H NMR at –65 °C.

Protonation of 12c: In a 5-mm NMR tube, 10 mg of a 1:1 mixture of cyclized **12c** and BcPh was introduced. The NMR tube was then flushed with argon, cooled to –78 °C and about 0.3 mL of SO_2ClF was condensed into it. After completion of SO_2ClF addition, 3–4 drops of FSO_3H were slowly added in order to avoid local overheating. The mixture immediately turned deep-blue. After vigorous stirring at –78 °C (vortex), 6–8 drops of CD_2Cl_2 were slowly introduced into the NMR tube (vortex mixing) and the sample was studied by NMR at –65 °C. Only resonances due to **12cH$^+$** were observed. As shown previously,[10] protonated BcPh can not be generated under persistent ion conditions (likely due to radical cation formation).

Supporting Information (see also the footnote on the first page of this article): Selected NMR spectra for the products and the carbocations and computational data (Figures S1–S15 and Tables S1–S2).

Acknowledgments

Support of our work in the PAH area under "reactive intermediates of carcinogenesis of PAHs" by the National Cancer Institute of the National Institutes of Health (2R15CA078235-02A1 and 1R15CA078235-01A1) is gratefully acknowledge.

[1] T. Okazaki, K. K. Laali, B. Zajc, M. K. Lakshman, S. Kumar, W. M. Baird, W.-M. Dashwood, *Org. Biomol. Chem.* **2003**, *1*, 1509–1516.
[2] K. K. Laali, S. Hollenstein, *J. Chem. Soc. Perkin Trans. 2* **1998**, 897–904.
[3] K. K. Laali, M. Tanaka, S. Hollenstein, M. Cheng, *J. Org. Chem.* **1997**, *62*, 7752–7757.
[4] K. K. Laali, P. E. Hansen, *J. Org. Chem.* **1997**, *62*, 580–5810.
[5] S. Hollenstein, K. K. Laali, *Chem. Commun.* **1997**, 2145–2146.
[6] K. K. Laali, T. Okazaki, R. G. Harvey, *J. Org. Chem.* **2001**, *66*, 3977–3983.
[7] R. G. Harvey, *Polycyclic Aromatic Hydrocarbons*, Wiley-VCH, New York, **1997**, pp. 140–143.
[8] K. K. Laali, P. E. Hansen, *J. Org. Chem.* **1991**, *56*, 6795–6803.
[9] K. K. Laali, S. Hollenstein, R. G. Harvey, P. E. Hansen, *J. Org. Chem.* **1997**, *62*, 4023–4028.
[10] K. K. Laali, T. Okazaki, S. Kumar, S. E. Galembeck, *J. Org. Chem.* **2001**, *66*, 780–788.
[11] C. Brulé, K. K. Laali, T. Okazaki, M. K. Lakshman, *J. Org. Chem.* **2007**, *72*, 3232–3241.
[12] R. G. Harvey, *Polycyclic Aromatic Hydrocarbons*, Wiley-VCH, New York, **1997**, pp. 153.
[13] W. Koch, M. C. Holthausen, *A Chemist's Guide to Density Functional Theory*, 2nd ed., Wiley-VCH, Weinheim, **2000**.
[14] M. J. Frisch, G. W. Trucks, H. B. Schlegel, G. E. Scuseria, M. A. Robb, J. R. Cheeseman, J. A. Montgomery Jr, T. Vreven, K. N. Kudin, J. C. Burant, J. M. Millam, S. S. Iyengar, J. Tomasi, V. Barone, B. Mennucci, M. Cossi, G. Scalmani, N. Rega, G. A. Petersson, H. Nakatsuji, M. Hada, M. Ehara, K. Toyota, R. Fukuda, J. Hasegawa, M. Ishida, T. Nakajima, Y. Honda, O. Kitao, H. Nakai, M. Klene, X. Li, J. E. Knox, H. P. Hratchian, J. B. Cross, V. Bakken, C. Adamo, J. Jaramillo, R. Gomperts, R. E. Stratmann, O. Yazyev, A. J. Austin, R. Cammi, C. Pomelli, J. W. Ochterski, P. Y. Ayala, K. Morokuma, G. A. Voth, P. Salvador, J. J. Dannenberg, V. G. Zakrzewski, S. Dapprich, A. D. Daniels, M. C. Strain, O. Farkas, D. K. Malick, A. D. Rabuck, K. Raghavachari, J. B. Foresman, J. V. Ortiz, Q. Cui, A. G. Baboul, S. Clifford, J. Cioslowski, B. B. Stefanov, G. Liu, A. Liashenko, P. Piskorz, I. Komaromi, R. L. Martin, D. J. Fox, T. Keith, M. A. Al-Laham, C. Y. Peng, A. Nanayakkara, M. Challacombe, P. M. W. Gill, B. Johnson, W. Chen, M. W. Wong, C. Gonzalez, J. A. Pople, *Gaussian 03*, Revision E.01, Gaussian, Inc., Wallingford CT, **2004**.
[15] K. K. Laali, T. Okazaki, P. E. Hansen, *J. Org. Chem.* **2000**, *65*, 3816–3828.
[16] M. Sarobe, L. W. Jenneskens, J. Wesseling, U. E. Wiersum, *J. Chem. Soc., Perkin Trans. 2,* **1997**, 703–708.
[17] M. Sarobe, H. C. Kwint, T. Fleer, R. W. A. Hevenith, L. W. Jenneskens, E. J. Vlietstra, J. H. Van Lenthe, J. Wesseling, *Eur. J. Org. Chem.* **1999**, 1191–1200.

Received: March 6, 2008
Published Online: June 11, 2008

